Spring 5-1-2015

Finite Element Analysis of the Application of Ultrasound-Generated Acoustic Radiation Force to Biomaterials

Nicole J. Piscopo
University of Connecticut - Storrs, nicole.piscopo@uconn.edu

University of Connecticut Honors Program

Finite Element Analysis of the Application of Ultrasound-Generated Acoustic Radiation Force to Biomaterials

Honors Scholar Thesis

Nicole J. Piscopo[1]

Thesis Advisor: Dr. Yusuf Khan[2]

Honors Advisor: Lisa Ephraim[1]

1 Department of Biomedical Engineering, University of Connecticut

2 Department of Orthopaedic Surgery, University of Connecticut Health Center

Table of Contents

1. Table of Figures

2. Table of Tables

3. Abstract

While most bone fractures can heal simply by being stabilized, others can take a longer time to rejoin or they could fail to merge back together completely. Numerous studies have shown the positive effects that ultrasonic therapy have had on delayed-union and non-union bone fracture repair but little is known as to what specific biological mechanisms are at play. Ultrasound may be a valuable tool for bone tissue regeneration at these fracture sites using a tissue engineering approach, however, more must be understood about its impact on stimulating tissues to heal before this can be a reality. For that reason, this study shows that it is possible to utilize an *in-silico* finite element analysis model to show both three-dimensional predictive hydrogel deformation and the displacement of beads and cells in the hydrogel from the ultrasound-generated acoustic radiation force. The model used for this is collagen based hydrogels seeded with pre-osteoblast cells and polystyrene beads. This is done in order to provide quantitative confirmation of real-time deformation imaging in a study showing the effect of remote physical forces provided by ultrasonic therapy on bone healing.

4. Introduction

Low intensity pulsed ultrasound (LIPUS) is an ultrasonic therapy currently in clinical use. In 1997, Cook et al applied LIPUS for 20 minutes a day to both distal radial and tibial fractures and saw a 41% and 51% reduction in healing time, respectively [1]. One possible mechanism for the effectiveness of LIPUS treatment may be related to the principles of osteoblast response to mechanical loading. Osteoblasts respond to physical forces such as fluid shear and substrate deformation by a myriad of responses, including an up-regulation of overall bone formation. Implanting naked osteoblasts to a bone defect to supplement traditional fracture repair treatment may enhance bone formation when combined with LIPUS, but also presents challenges associated with cell retention at the defect site. Using hydrogels to prevent cells from drifting away from the defect site may circumvent these problems, but only if the LIPUS generated mechanical loading is transferred to the cells within the hydrogel. If so, it can be surmised that physical forces applied to the hydrogel would translate to the osteoblasts and manifest themselves similarly to those seen from other mechanically applied forces. By applying a low level force to the hydrogels, it is a reasonable hypothesis that cells would undergo either deformation and/or deflection in different directions as the hydrogel deforms due to the mechanical stimulus. In an effort to provide more insight to the mechanisms at hand during the ultrasonic treatment, this work will describe how the acoustic radiation force felt by these cells seeded in a hydrogel will be modeled through the use of finite element analysis.

4.1 Bone Physiology

Bone is between 50-70% mineralized matrix, 20-40% organic matrix, and the remainder is comprised of water and lipids [2]. Hydroxyapatite (HA) [$Ca_{10}(PO_4)_6(OH)_2$] makes up most of the mineral component. The extracellular matrix (ECM) of bone is comprised of mostly

collagenous proteins but the non-collagenous proteins include osteocalcin, osteopontin, and bone salioprotein [2].

The two main types of bone tissue are compact bone and spongy bone. The compact, or cortical, bone is made up of smaller bone units called osteons which are a key component of the larger Haversian system, seen in Figure 1. The Haversian system consists of a hard matrix of concentric lamellae. In between the lamellae are lacunae which are spaces occupied by bone cells called osteocytes. Small canaliculi are also present to function as canals that connect each lacunae to one another and to the central canal in the long bone to provide nutrients to the cells throughout the osteon. Spongy bone, or trabecular bone, follows a similar pattern of physiology except it lacks a central canal and their osteons are called packets. Instead of the cylindrical shape found in the compact bone along a central canal, the trabecular bone also has numerous thin rods of bone dispersed in different orientations throughout the bone marrow compartment [2].

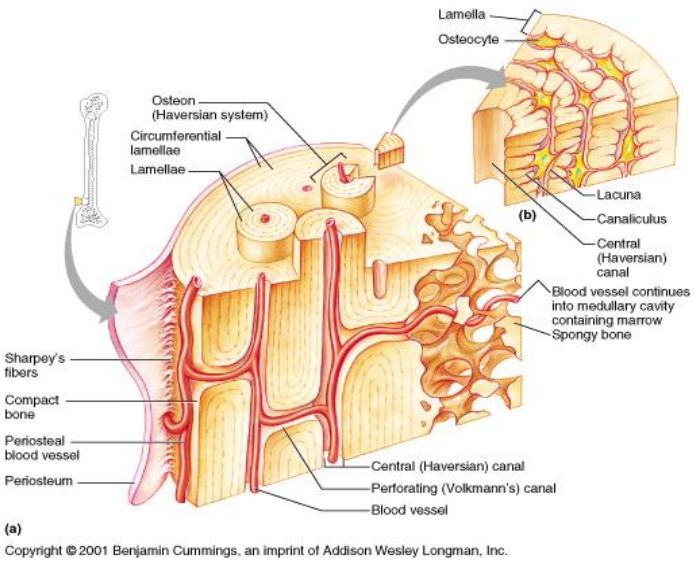

Figure 1. The organization of the structure of bone. The bottom left of the picture shows the macro scale organization of bone while the zoomed in section shows the micro scale organization of the bone [3].

Bone homeostasis is maintained by two important types of cells in bone, osteoblasts and osteoclasts [4]. Together, they are responsible for the dynamic response of bone from external forces. Osteoblasts are known for secreting new bone minerals into the matrix while osteoclasts are responsible for the process known as bone resorption in which the bone matrix is broken down. When people exercise in ways such as running or lifting weights, they add additional stresses to their bones and the osteoblasts secrete more bone matrix in order to withstand these increasing forces. When people are less active, their osteoblasts do not produce new bone matrix as quickly as their osteoclasts are breaking up the organic bone minerals.

When bone cannot withstand the forces being applied to it, fracture occurs. The natural healing process of bone involves three stages, inflammation, repair, and remodeling [5]. During inflammation, a hematoma, a swelling due to a break in a blood vessel, develops which recruits numerous cell types including macrophages, monocytes, lymphocytes, polymorphonuclear cells, and fibroblasts. As a result of the activities performed by the recruited cell types, granulation tissue forms. At this point, new vasculature begins to form to allow for nutrients and oxygen to flow into the fracture site. In the repair stage, capillaries continue to grow. With proper immobilization, a collagen matrix can be laid down that provides for osteoid secretion which can then be mineralized to form a soft callous. This callus then begins to calcify into the remodeling stage where the bone is reshaped and eventually reaches its original structure and mechanical strength [5].

4.2 Acoustic Radiation Force

An ultrasound transducer is capable of producing a sound wave at a varied range of amplitudes and frequencies. The system works by converting an electrical signal from the power source into a mechanical one by the rapid motion back and forth of the head of the transducer. It

is this movement that allows for a mechanical wave to be propagated. Since sound is the rapid motion of molecules, the ultrasound produces an acoustic wave [6]. As this acoustic wave propagates, it applies a radiation force through the medium in which it is moving and can transmit that force to any objects in the medium that it may come in contact with along the way. The wave produced from an ultrasonic transducer head is often represented by a sine wave as seen in Figure 2. The peak of the wave represents when the transducer head mechanism is fully extended and the trough of the sine wave represents when the transducer head mechanism is retracted.

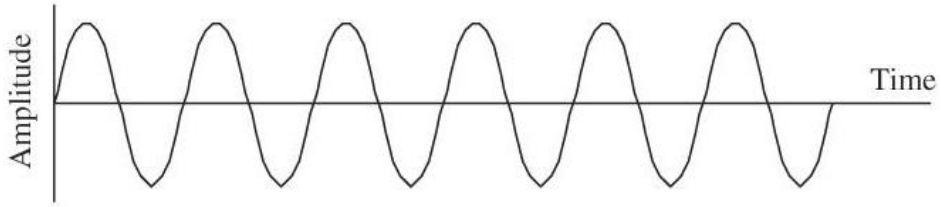

Figure 2. A continuous sine wave representation of an ultrasonic wave [2].

Another type of acoustic wave is a pulsed wave. A pulsed wave is not a continuous waveform like in Figure 2. Instead, the signal is turned on for a limited span of time, or pulsed, and then turned off. The repeated change in signal creates a pulsed wave as is shown below in Figure 3.

Figure 3. A pulsed sine wave in which the signal is turned off and on.

Currently, the FDA has approved of a LIPUS in which the therapy is applied for 20-minutes daily, at a 1 MHz or 1.5 MHz carrier wave, 1 kHz pulse rate frequency, 20% duty cycle,

and an average intensity of 30 mW/cm^2 [7]. The 20% duty cycle means that for every 1000 Hertz, the signal is turned on for 200 Hertz and off for the remainder 800 Hertz. These are the parameters the ultrasound is set to during our *in-vitro* hydrogel studies.

4.3 Mechanotransduction

Due to the turnover of the bone matrix in response to outside physical forces, the acoustic radiation force provided by the ultrasonic transducer may have the ability to stimulate bone growth in otherwise dormant bone fracture sites [8]. The dynamic destruction and repair of bone in response to an applied external force, in this case an acoustic radiation force, is explained by a process known as mechanotransduction, the process by which force is transferred from the environment into cells and is converted into a biochemical signal [9]. In the case of the osteoblast, it is through the appendages which they use to adhere to the bone matrix. The law governing the bones response to these forces is Wolff's Law which states that bone is rebuilt in response to the forces that act upon it [10]. In order for Wolff's Law to be true, mechanotransduction must take place. Mechanotransduction can occur through a number of one or more ways, including through adhesions or cytoskeleton elements, as can be seen in Figure 4. When osteoblasts are seeded into a hydrogel, it is understood that these appendages stretch out to

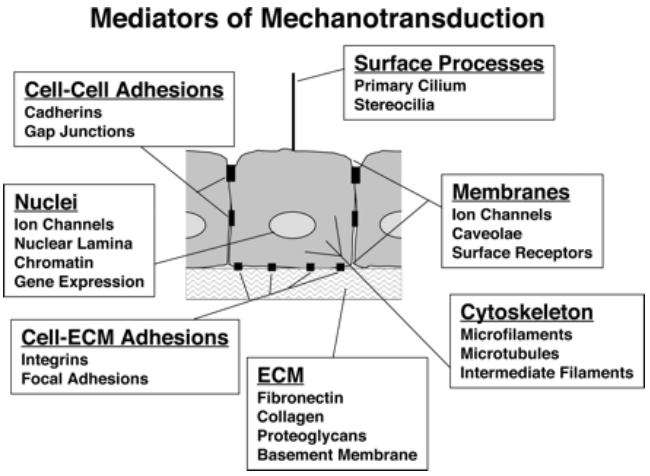

Figure 4. The mechanisms by which mechanotransduction can propagate from an external force into the cellular environment. These forces can be transmitted through surface processes, cellular adhesions (both cell to cell and cell to ECM), through membranes, through the ECM, the cytoskeleton, and the nucleus itself. [9].

hold the cells in place once again. By applying a low level acoustic radiation force to the hydrogels via ultrasound, physics implies that the cells' appendages would undergo a tugging in different directions as the hydrogel deforms due to the mechanical stimulus. It is this cyclic tugging force experienced by the cells that is theorized to be the cause for the biological changes observed.

4.4 Finite Element Analysis

Finite element analysis is a computational technique that can be used to calculate a system of differential equations across a geometric model. It works via constructing a mesh across the structure of interest by placing a number of nodes throughout the model and connecting them with a series of straight lines to form tetragonal geometries. The program then calculates the solutions to the differential equations generated at each of the nodes and produces a heat map of the different stresses, strains, or displacements at the different node locations. By summing all of these calculations across the model, it can be seen how different parts of the whole design will react when a given force is applied. COMSOL Multiphysics 4.4, a finite element analysis software package, can be utilized to model our system by predicting both hydrogel deformation as well as the force felt by the cells seeded in the hydrogel resulting from the ultrasound transducer. In our studies, the COMSOL Acoustics Module was applied to geometries mimicking our *in-vitro* setup with applied material properties to match the hydrogel, preosteoblast cells, and polystyrene beads.

5 Materials and Methods

5.1 Computational Materials

The software used in this study is COMSOL Multiphysics version 4.4. COMSOL is a graphical user interface that allows for the user to apply different and numerous physics

modules, such as structural mechanics, chemistry, or acoustics, to a user defined geometry with a set of specified material properties. The software allows the user to define the parameters for their own mesh to be placed over the geometries to be simulated and then generates and solves the associated differential equations at each of the nodes in the mesh.

For this study, the Acoustics Module was utilized to model the transmission of the simulated ultrasonic acoustic wave through the water in the 6-well plate that held the hydrogel during the *in-vitro* study. This then allowed for the displacement of the pre-osteoblast cells and polystyrene beads, used to allow real time visualization of the hydrogels in bench-top testing, to show how the cells and beads displace in relation to one another inside of the hydrogel as well as the deformation of the hydrogel itself when the ultrasonic force was applied.

5.2 *In-vitro* Materials

The following materials are used for the bench top *in-vitro* studies that the computational simulations are modeled after. While it is important to understand the *in-vitro* need for each of these components, it is vital for the computational simulation to know the properties of each of the individual materials to track how the acoustic radiation force propagates through them.

5.2.1 Collagen-Based Hydrogels

Hydrogels are 3D cross-linked porous hydrophilic networks often used in tissue engineering [11]. One purpose of hydrogels is drug delivery. When hydrogels are exposed to water, they swell and then release their contents into the surrounding environment. In the *in-vitro* studies being mimicked here, the hydrogel serves as a cell carrier to contain the seeded cells in a fixed location such as to prevent the cells from drifting out of the bone fracture zone and out of the range of the acoustic radiation force. Due to the ability for hydrogels to be made out of

various materials, both organic and inorganic, they can be used to mimic numerous types of extra cellular matrix environments [11].

The hydrogels used in the *in-vitro* studies here are collagen based to mimic the bone ECM environment. To create a hydrogel, Phosphate Buffer Solution (PBS), 1M NaOH, α-Minimum Essential Medium (α-MEM), and Rat Tail Collagen Type 1 are all mixed on ice. When seeding cells into the hydrogel, at this time, only half of the cells should be added to the solution and mixed. The hydrogel solution is then pipetted into a well plate and allowed to gel for 30 minutes at 37°C. Once the hydrogel has formed, the remainder half of the cells are then pipetted on top of the hydrogel. This is done because when all of the cells are added at the initial time of mixing the hydrogel solution, the cells have a tendency to sink in the forming hydrogel. By adding the cells at two different times a more even distribution of cells is achieved throughout the thickness of the hydrogel.

5.2.2 MC3T3 Pre-osteoblasts

MC3T3 cells are fibroblast like cells that are derived from the calvaria of the mouse C57BL/6 strain [12]. They are pre-osteoblast cells that are often used *in-vitro* to model osteoblast differentiation via ECM signaling [13]. In the *in-vitro* studies, the MC3T3 cells are stimulated to differentiate by the 1 MHz carrier frequency pulsed at 1 kHz with a 20% duty cycle at 30mW/cm^2 intensity which is applied for 20 minutes for either 1, 3, or 7 days. The mRNA is then extracted from the cells that were seeded in the hydrogels and reverse transcriptase quantitative polymerase chain reaction (RT-qPCR) is performed to analyze the change in levels of osteogenic genes on a transcriptional level.

5.2.3 Polystyrene Beads

To monitor the deformation of the hydrogels under the pulsed ultrasonic acoustic force, 2μm Fluoro-Max™ Red Flourescent Polymer Microspheres from ThermoScientific were seeded into the hydrogels, which are otherwise not visible during testing. In previous studies, the encapsulated fluorescent beads were imaged under the acoustic force using a Nikon optical microscope equipped with epifluorescence, and a water-cooled digital camera (Hammamatsu, Inc.). These images, seen below in Figure 5, were then collected and analyzed using Volocity Software, (Improvision, Inc.). The results of these studies showed that the beads underwent a displacement inside of the hydrogel when the ultrasonic signal was applied.

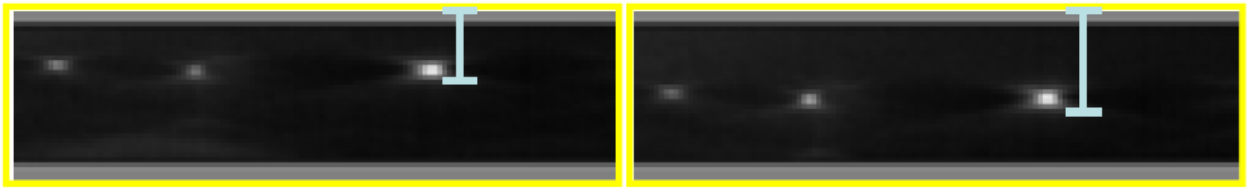

Figure 5. The left picture shows the depth of a fluorescent bead in a collagen hydrogel. The right image then shows the new depth of that same bead during the portion of the ultrasonic therapy cycle when the acoustic force is applied (unpublished data).

5.3 Methods

The following Finite Element Analysis COMSOL simulation was based on the design of a pre-existing Acoustic-Structure Interaction Model provided by the COMSOL Model Library with specific parameter modifications to mimic our *in-vitro* study [14].

5.3.1 How to Create a FEA Model in COMSOL

Upon opening COMSOL version 4.4 and starting a new model, the "Model Wizard" option was selected followed by "3D" in Space Dimensions of the Model Wizard Window. The next step was then to select the Physics Module to add to the model. In the Module Window, "Acoustics" was selected, followed by "Acoustics-Structure Interaction", and then "Acoustic-

Solid Interaction, Frequency Domain" was added to the model. Then, in Preset Studies, "Frequency Domain" was selected to finish specifying what types of simulations were run.

The next step was to construct the geometries for the model. The following description will describe how the geometries seen in Figure 6 below were constructed. In the Model Builder Window, the "Geometry" node was clicked and the units were set to centimeters. "Geometry" was then right clicked and "+Cylinder" was selected. The first cylinder represents the media that the hydrogel sits in while it is in the well plate. For the media cylinder, the type was left as "Solid". The radius was then set to 1.1cm and height to 0.8cm. The x, y, and z positions were left at 0 which placed the center of the bottom of the gel at the origin. "Build All" was then clicked at the top of the window which caused the cylinder to appear in the Graphics window. This cylinder was then renamed as "Media". Renaming the geometries made it easier to assign them boundary conditions later on. The shape of the hydrogel was approximated to be a cylinder and thus another cylinder was added to the model by right clicking on "Geometry" and selecting "+Cylinder". This cylinder's radius was set to 1cm, height to 0.6cm, and the x, y, and z positions were left at 0. "Build All" was then selected again and the result was one cylinder inside of the other. This second smaller cylinder was renamed to "Hydrogel".

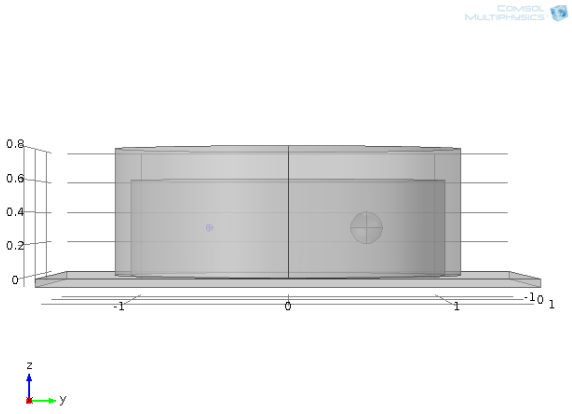

Figure 6. The COMSOL geometric simulation of the *in-vitro* test setup.

Most of the computational studies that were conducted here involved comparing and contrasting the response of a cell inside of the hydrogel to that of a polystyrene bead inside of the gel under the ultrasonic force. To create a bead, "Geometry" was clicked on in the left hand drop down menu and "+Sphere" was selected. The beads used in the *in-vitro* study had a 2μm diameter so 0.0001cm was input for this radius. However, when constructing the meshes around the geometries at a later point in the computational model, there is a lower limit to the minimum mesh size that can be generated around such a small geometry. As a result, the smallest spherical geometry that would yield results was tested and found to have a radius of 0.02cm. For position, the x was left at 0cm, the y was set to -0.5cm, and the z was set to 0.3cm (see Figure # for axes orientation). Clicking "Build All" placed the bead on the left hand side of the hydrogel. This sphere was then renamed to "Bead".

To create a cell, "Geometry" was right-clicked in the left hand drop down menu and "+Sphere" was selected. According to Sugawara et. al. the average diameter for an osteocyte is about 10μm [15]. It was noted that the smallest sphere that could be generated with the software had a radius of 0.02cm. Rather than model cells and beads with geometric spheres of the same size (which are not the same size in reality) the cell was scaled to remain 5 times the size of the bead, to approximate the difference between a bead and a real cell. Therefore, the cell radius was set to 0.1cm. For the position, the x was left at 0cm, the y was set to 0.5cm, and the z was set to 0.3cm which placed the cell on the right hand side of the gel. After selecting "Build All", a cylinder, the culture dish, with another cylinder inside of it, the gel in the culture dish, and two spheres, one 5 times the size of the other, was generated as depicted in Figure 6. This sphere was then renamed as "Cell".

Next the material properties, which permitted different geometries to be added to the model, were selected. A right-click on "Materials" in the left dropdown menu and a click on "+Material" completed this function. This created a new material under the "Materials" node. In the "property Group" Window, the "Output Properties" node was selected. Numerous properties then drop down and in order for a simple run, it was necessary to add Density, Poisson's Ratio, and Young's Modulus. To add them, they were clicked on and the "+" button below was selected. The two preexisting materials in the Materials Library that were used were Water and Polystyrene. The Water material was then applied to the Media geometry domain and the Polystyrene material was applied to the Bead domain. This ensures that the properties associated with water and polystyrene are applied to the media and the bead, respectively.

Two materials needed to be custom made. In the Materials Library, "Add New Material" was selected. This first material was for the hydrogel. The Young's modulus of a hydrogel was previously measured and reported to be 1500 Pa (unpublished data). The density was calculated to be 1200 kg/m^3. The Poison's ratio was set to 0.499 because the hydrogel is mostly water and therefore highly incompressible. Finally, the speed of sound in a hydrogel was set to 1480 m/s which is actually the speed of sound in collagen gel which is a reasonable approximation. Once this material was defined, it was applied to the Hydrogel geometry domain. The final material to be defined was that which was applied to the cell. For the cell, the only material properties needed were the density, which according to Sagawara et. al. is 1.06 kg/m^3, and the speed of sound which was assumed to be the same as water, 1500 m/s, due to the contents of the cell [16].

Once the geometries were defined and their material properties are assigned, it was important to set the Global Definitions and the Boundary Conditions. The global definitions control the frequency at which the ultrasonic signal will be simulated and the remainder

parameters defined the direction of the signal. In the drop down menu “Global Definitions” was selected and then “Parameters” was double clicked. The values in Table 1 were then input. The value of f can be changed given the type of simulation that would like to be run. It was left at 1Hz for these trials because when run, that frequency produced a snap shot of the ultrasonic signal being applied. Phi was 0 radians because the direction in which the signal is being applied from was directly above the hydrogel and theta was π radians because the signal was travelling downward onto the hydrogel and from 0 to π is 180 degrees, or a straight line in the downward direction. The values of k1, k2, and k3 were then calculated based on the phi and theta values such that k1 became a number extremely close to 0, k2 became 0, and k3became -1. This correlated with the signal only travelling down in the negative z direction and not in the x or y directions.

Name	Expression	Description
F	1[Hz]	Frequency of ultrasonic signal
Phi	0[rad]	Wave direction angle
theta	pi[rad]	Wave direction angle
k1	sin(theta)*cos(phi)	Incident wave direction vector, X component
k2	sin(theta)*sin(phi)	Incident wave direction vector, Y component
k3	cos(theta)	Incident wave direction vector, Z component

Table 1. This table represents the input values for the Parameters in the Global Definitions.

The boundary conditions must also be set such that the simulation could respond to different types of barriers between different materials. In “Definitions” of the Model Builder Window, “Selections” was right-clicked followed by “Explicit”. In the Domain selection, the Media geometry was chosen and renamed as the “Fluid Domain”. Again, in “Definitions” of the Model Builder Window, “Selections” was right-clicked followed by “Explicit” and this time the Hydrogel geometry was selected for the domain. This domain was then renamed as “Solid Domain”. Finally, one more Explicit was created and this time the “All Domains” box was highlighted. In the “Output Entities” list, “Adjacent boundaries” was selected and renamed to

"Radiation Boundaries". This allowed for the ultrasonic signal to travel through all entities in the simulation.

The last required condition to be set was the fixed constraint at the bottom of the hydrogel. The "Solid Mechanics" node was right clicked and then "+Fixed Constraint" was chosen. In boundary selection, "Manual" was highlighted and in the Graphics window, the bottom surface of the cylinder was established as the Fixed Constraint. This told the program to run as if the bottom of the gel would have no displacement when the force is applied.

The final step before running the simulation was constructing the Mesh on which the simulation would be run. The "Mesh" node was right clicked in the Model Builder Window followed by the "+Free Tetrahedral". In "Geometric entry level", the "Entire geometry" was chosen. Due to the fact that the signal was being applied to very small geometries such as the bead, a custom mesh size was required to be selected. Double clicking on the "Size" branch of the left drop down menu brought up the size parameters for the mesh. Selecting "Custom" caused another branch to open which included element size parameters such as Maximum element size, Minimum element size, Maximum element growth rate, Curvature factor, and Resolution of narrow regions.

The Maximum element size parameter limits the size of the tetrahedral that may form. In this simulation, the maximum size was set to 5000[m/s]/f/5 which made the mesh such that it was large enough to allow for 5 elements of the mesh per wavelength. The minimum element size was then changed such that it was not larger than the maximum size. In this case, the minimum element size was set to 1e-17 cm to produce very fine structures that allowed for the simulation to appropriately detail the deformation of the small beads. The maximum element growth rate, curvature factor, and resolution of narrow regions were then left at the predefined

values which were 1.4, 0.4, and 0.7 respectively. “Build All” was then selected at the top bar and a mesh appeared over the cylinder of the Graphics window.

At this point, the file was saved before the simulation was run. To run the simulation, the “Study” branch was selected and then the “Compute” button was clicked. The result then produced a displacement heat map as can be seen in Figure 7.

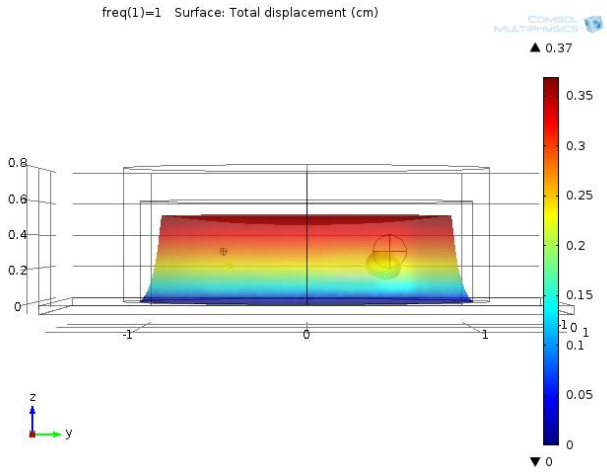

Figure 7. The result of the graphics window after running the simulation described.

5.3.2 Hydrogel Deformation Study

In the hydrogel deformation study, there was no need to place any beads or cells in the hydrogel. The hydrogel and the media cylinder were kept the same size and the material properties of both geometries remained the same as was previously described. This created a model as is seen below in Figure 8. For this study, three trials were run and the frequency of the applied signal was changed each time. Frequencies of 1MHz, 1kHz, and 1Hz all were run to analyze the different ways in which the hydrogel responded.

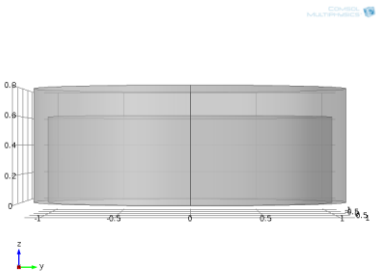

Figure 8. The model set up for the hydrogel deformation study in COMSOL. Scale is in centimeters.

5.3.3 Bead and Cell Displacement Study

In the bead and cell displacement study, two separate files needed to be constructed with one having a hydrogel containing beads and the other file having a hydrogel with cells. The hydrogel and media cylinder for both simulations were the same as in the hydrogel displacement study. In one of these new files, the hydrogel was filled with nine spheres in three rows of three at the same size and material properties of the bead as can be seen in Figure 9 below. In the other new file, the hydrogel was filled with six spheres in two rows of three at the same size and material properties of the cells as can also be seen in Figure 9. The study that was conducted to analyze the displacement of the beads was run at 10 Hz.

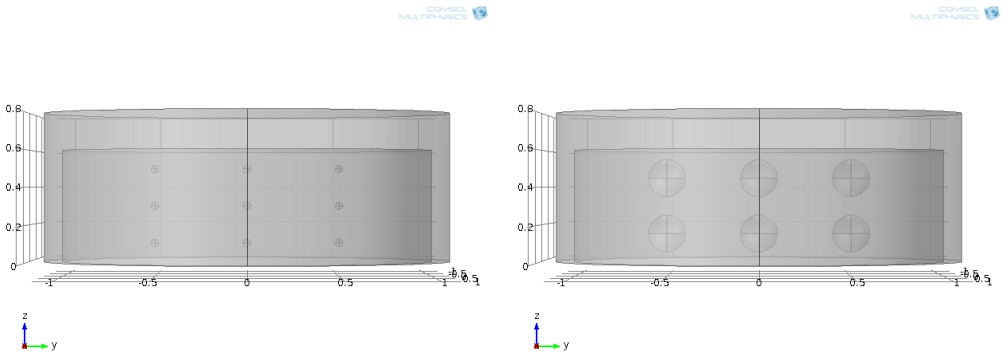

Figure 9. The left picture is the model of the nine polystyrene beads in the hydrogel in the media. The right picture is the model of the six cells in the hydrogel in the media.

5.3.4 Material Property Study

The model for the material property study involved the hydrogel inside of the media cylinder with two spheres of the same size inside of the hydrogel, one on each side. One of these spheres was given the material properties of the cell and the other was given the material properties of the bead as described above (see "How to Create a FEA Model in COMSOL" section). In this study, the frequency was kept constant at 1 Hz but in each simulation, the material properties were changed. The Young's Modulus, speed of sound, Poisson's Ratio, and density were changed to values both above and below the set values for the hydrogel. The measured output was the maximum displacement of the hydrogel.

6. Results

6.1 Hydrogel Deformation Study

In the hydrogel deformation study, frequencies of 1MHz, 1kHz, and 1Hz all were run to analyze the different ways in which the hydrogel responded. The simulation on the left of Figure 10 shows how the hydrogel deformed at a frequency of 1Hz. This was also the result when the simulation was run at 10 Hz. There was a maximum displacement of 1.68 nm which was experienced at the top of the hydrogel. When looking at the displacement heat maps, it is important to note that the actual distance shown between the original outline and the new deformed geometry is dramatized.

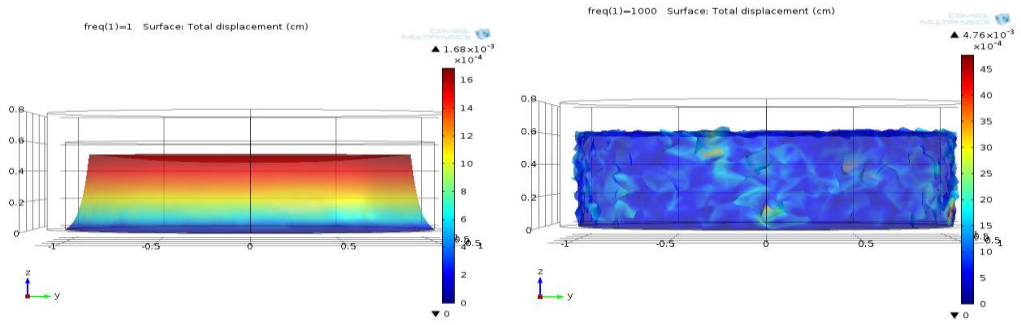

Figure 10. Left) The simulation run at a frequency of 10 Hz. Right) The simulation run at 1 kHz.

The Image on the right of Figure 10 shows how the hydrogel deformed at a frequency of 1kHz. The maximum deformation at 1 kHz was 4.76 nm which did not occur in just one localized location such as was shown in the 1 Hz simulation. Based off of these results, running the simulations at lower frequency such as 1 or 10 Hz will provide a better representation of the displacement that occurs on the 20% on portion of the duty cycle during the LIPUS signal application.

6.2 Bead and Cell Displacement Study

In both the bead and cell displacement studies, the frequency that the simulations were run at was 10 Hz. The simulations were run, however, at three different hydrogel densities which were 600kg/m^3, 1200kg/m^3, and 1800kg/m^3. The 1200kg/m^3 density was chosen because this was the experimental density. The 600kg/m^3 and 1800kg/m^3 densities were chosen to show a larger range of densities to expose the effect of change in density of the bead and cell displacements. The results for this can be seen in Table 2.

In Table 2A, the cell seeded hydrogel with a density of 600kg/m^3 has a maximum displacement of 400nm. Table 2B describes the maximum displacement for the cell seeded hydrogel with a density of 1200kg/m^3 as 500nm. 500nm is also the maximum displacement for the cell seeded hydrogel with a density of 1800kg/m^3 which is shown in Table 2C. In Table 2D, the bead seeded hydrogel with a density of 600kg/m^3 has a maximum displacement of 0.5cm. Table 2E shows the maximum displacement for the bead seeded hydrogel with a density of 1200kg/m^3 is 0.53cm. Finally, 0.49cm is the maximum displacement for the bead seeded hydrogel with a density of 1800kg/m^3 which is shown in Table 2F.

Cells	Beads
A. 600kg/m^3 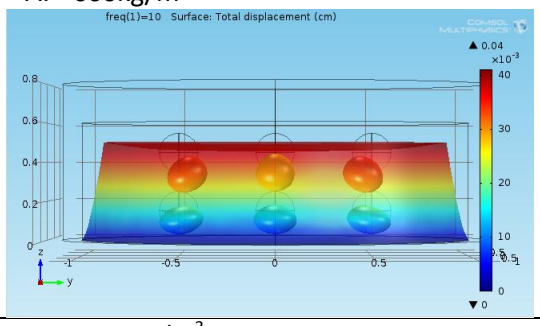	D. 600kg/m^3 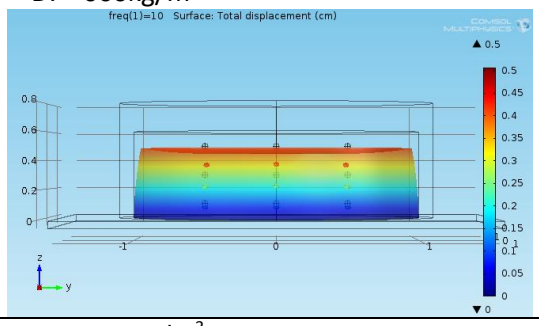
B. 1200kg/m^3 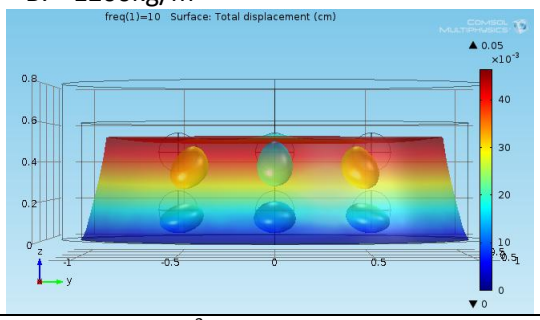	E. 1200kg/m^3 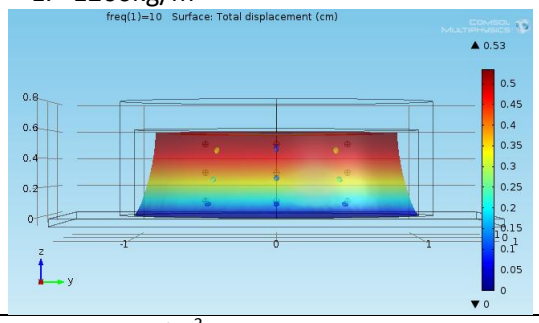
C. 1800kg/m^3 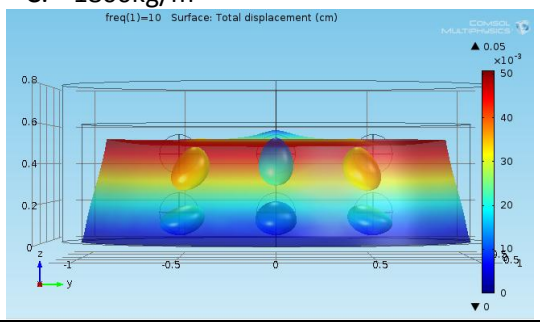	F. 1800kg/m^3 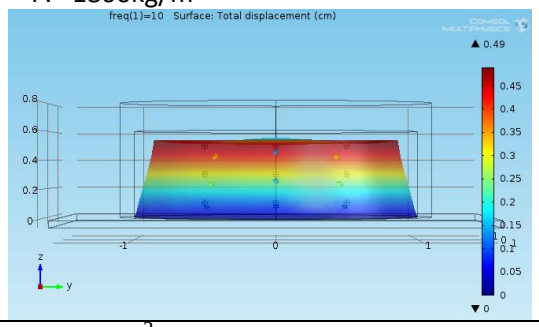

Table 2. A) The cells in the hydrogel at a density of 600 kg/m^3. B) The cells in the hydrogel at a density of 1200 kg/m^3. C) The cells in the hydrogel at a density of 1800 kg/m^3. D) The beads in the hydrogel at a density of 600 kg/m^3. E) The beads in the hydrogel at a density of 1200 kg/m^3. F) The beads in the hydrogel at a density of 1800 kg/m^3.

When looking at the pseudocolor imposed on each image, with red indicating the most movement and blue the least, describing the movement within the hydrogel, it can be seen that the cells and beads near the top of the hydrogel exhibit more displacement than the contents on the bottom of the hydrogels.

6.3 Material Property Study

To determine the importance of the different material properties in the displacement of the hydrogels, multiple trials where run and in each trial, one of the material properties of the hydrogel was altered while the others remained constant. Table 3 shows the results.

Hydrogel Properties	Young's Modulus (Pa)	Speed of Sound (m/s)	Poisson's Ratio	Density (kg/m3)	Displacement Min (mm)	Displacement Max (mm)
Trial 1	1,500	1,480	0.48	1,200	2.45E-08	8.11E-07
Trial 2	1,500	**1,000**	0.48	1,200	2.29E-08	7.25E-08
Trial 3	1,500	**100**	0.48	1,200	1.63E-10	5.16E-09
Trial 4	1,500	**2,000**	0.48	1,200	9.34E-09	2.80E-07
Trial 5	1,500	**10,000**	0.48	1,200	1.43E-08	5.24E-07
Trial 6	**1,000**	1,480	0.48	1,200	2.54E-08	8.11E-07
Trial 7	**100**	1,480	0.48	1,200	2.54E-08	8.11E-07
Trial 8	**2,000**	1,480	0.48	1,200	2.54E-08	8.11E-07
Trial 9	**10,000**	1,480	0.48	1,200	2.54E-08	8.11E-07
Trial 10	1,500	1,480	**0.4**	1,200	2.54E-08	8.11E-07
Trial 11	1,500	1,480	**0.3**	1,200	2.54E-08	8.11E-07
Trial 12	1,500	1,480	0.48	**1,000**	2.91E-08	9.69E-07
Trial 13	1,500	1,480	0.48	**1,500**	1.98E-07	6.51E-07

Table 3. The results of altering the different material properties run at a frequency of 1 Hz.

Changing the speed of sound of the hydrogel altered the displacement of the hydrogel. There was no direct correlation, however, between an increase in speed of sound and the range of displacement values seen by the hydrogel. Altering the Young's Modulus and the Poisson's Ratio of the hydrogels do not change the displacement values of the hydrogel. Finally, changing the density of the hydrogel also altered the displacement range exhibited during the applied frequency. A higher density, such as 1,500 kg/m^3, had a displacement range of 5.34 nm as compared to 1,000 kg/m^3 which had a displacement range of 7.87 nm indicating that there was a negative correlation between the density and displacement.

7. Discussion

7.1 Hydrogel Deformation Study

The results from the hydrogel deformation study show a Finite Element Analysis simulation can successfully model the response of the hydrogel under the influence of an ultrasonic force. In comparing the differences between the two simulations shown in Figure 10, it can be seen that the most optimal way to mimic the deformation after one on cycle of the ultrasonic force is at 10 Hz. At the higher frequency, the result appears to be summation of the entire on and off cycles which makes it more difficult to see the impact that just 1 cycle would create as just 1 step in the process. For this reason, the remainder of the studies were simulated at a frequency of 10 Hz.

7.2 Bead and Cell Displacement Study

In the *in-vitro* studies in which the encapsulated fluorescent beads were imaged under the acoustic force (data not shown), only the beads on the bottom portion of the hydrogel could be imaged. By using the information provided by the COMSOL simulations in the Bead and Cell Displacement Models, it can be seen that the beads and cells on the top portion of the hydrogel undergo a larger displacement than those on the bottom. This makes the COMSOL model an important tool in fully understanding the nature of the bead displacement throughout the entire height of the hydrogel.

It is important to verify the model results with *in-vitro* testing in which the cells in the hydrogel that have been exposed to the ultrasonic forces were isolated from the gel such that the top and bottom of the gel were separated and then evaluated using assessment techniques such as rt-PCR on each population separately. These results could provide more information as to

whether or not the difference in the forces felt by the top cells versus the bottom cells would impact the distribution of bone formation or the rate at which it may form.

7.3 Material Property Study

The results of the material property study show that the speed of sound and the density of the hydrogel both impact hydrogel deformation. The Poison's Ratio and the Young's Modulus did not influence the deformation when they were altered. The density of the hydrogel is a factor that would be easy to modify *in-vitro* as more collagen would simply need to be added to the solution while preparing the hydrogel. In the future, it may be possible to find an optimal density of the hydrogel for enhanced cell response by comparing the collagen concentration with the results of the rt-PCR. Also, since the speed of sound is a property that is dependent on the density of the medium through which the sound is traveling, the density can be considered the most important factor in determining how much force the cells feel during the ultrasonic radiation force and thus in the *in-vitro* studies, the density of the collagen hydrogels can be varied.

8. Conclusion

In conclusion, the COMSOL Finite Element Analysis simulations presented here demonstrate that the deformations of collagen based hydrogels under an applied ultrasonic radiation force can be predicted when taking into account their material properties. Simulations should be run at a frequency of 10Hz to best model the displacement of a single duty cycle of the ultrasonic therapy. The cell and bead displacement studies showed that the cells and beads on the top portion of the hydrogel witnessed more displacement than the cells and beads on the bottom. Additionally, the density of the hydrogel is the most important factor in determining the

deformation of the hydrogel and sub sequentially, the displacement of the beads and cells seeded in the hydrogel.

9. Future Applications

A worthwhile follow-up study could be conducted based off of the combined the results seen in the Bead and Cell Displacement Study, which included that the cells at the different heights in the hydrogel witnessed varying levels of displacement, and the Material Property Study, which showed that the density is the most influential property in predicting the deformation of the hydrogel. This study would involve creating one hydrogel comprised of three different layers. Each layer would have an increasing collagen density, from bottom to top, creating a density gradient in the z direction. The density of cells seeded in each of the layers would not change. The reason for the direction of this gradient is that in the Material Property Study, the lower densities witnessed more displacement, and in the Bead and Cell Displacement Study, the beads and cells on the bottom portion of the hydrogel had less displacement than those on the top. By placing the lowest density (which would have the highest displacement) on the bottom (where less displacement was predicted) the cells throughout all three layers of the hydrogel should witness a more uniform displacement.

In order to see if any statistically significant changes occur, it would be necessary to also measure the response of the cells in three separate hydrogels which are comprised of three layers, all with the same collagen density, but with cells only seeded in one of the layers. The cells should be present in the one layer that the correct density is found in the test hydrogel. For example, in the hydrogel with three of the densest layers, the cells should be seeded in the top layer only because the densest layer is found on the top of the test hydrogel. The schematic for this can be seen in Figure 11.

Figure 11. a) The test hydrogel in which each of the three layers have different densities but all three layers have cells seeded. b) The hydrogel has the highest density level and cells seeded in the top layer. c) The hydrogel has the medium density level and cells seeded in the middle layer. d) The hydrogel has the lowest density level and cells seeded in the bottom layer.

If this experiment can successfully create a uniform cellular response in the test hydrogel, this idea could be vital to designing better hydrogels for implantation to get a more uniform bone formation response *in-vivo*.

Furthermore, this type of modeling system of the ultrasonic technology is important for bone repair but can be applied to other test beds as well. For instance, the role of mechanical forces is currently being studied in the realm of both nervous and brain tissue. While it is known that traumatic injury or intense physical forces that brain cells feel during impact may lead to concussions, not much is known about how these tissues respond *in-vitro* three-dimensional models. The hydrogel and acoustic radiation force would be a good model for brain tissue and allow for chronically developing conditions to be monitored.

10. Acknowledgements

I would like to thank Dr. Yusuf Khan at the University of Connecticut Health Center for his guidance these past two years and throughout this research project. I would also like to thank James Veronick for his mentorship while working on this part of his project and the rest of the graduate students in Dr. Khan's lab for their help along the way.

References

[1] S.D.P. Cook, J.P. Ryaby, J.R. McCabe, J.J.P. Frey, J.D.M. Heckman and T.K.M. Kristiansen, "'Ovid: Acceleration of Tibia and Distal Radius Fracture Healing in Patients Who Smoke." *Clinical Orthopaedics and Related Research*, vol. 337, April, pp. 198-207.

[2] Clarke, "'Normal Bone Anatomy and Physiology," *Clinical Journal of the American Society of Nephrology*, vol. 3, no. Supplement 3, pp. S131-S139.

[3] J. Thompson, "'Bone Healing,".

[4] Tanaka, Nakayamada and Okada, "'Osteoblasts and Osteoclasts in Bone Remodeling and Inflammation," *Current Drug Target -Inflammation & Allergy*, vol. 4, no. 3, pp. 325-328.

[5] I. Kalfas, "'Principles of Bone Healing," *Neurosurgical Focus*, vol. 10, no. 4.

[6] OBRIENJR, "'Ultrasound–biophysics mechanisms☆," *Progress in Biophysics and Molecular Biology*, vol. 93, no. 1-3, pp. 212-255.

[7] Bhandari, Dijkman and Sprague, "'Low-intensity pulsed ultrasound: Nonunions," *Indian Journal of Orthopaedics*, vol. 43, no. 2, pp. 141.

[8] Bhandari, Mundi, Petis, Kaloty and Shetty, "'Low-intensity pulsed ultrasound: Fracture healing," *Indian Journal of Orthopaedics*, vol. 43, no. 2, pp. 132.

[9] Ingber, "'Cellular mechanotransduction: putting all the pieces together again," *The FASEB Journal*, vol. 20, no. 7, pp. 811-827.

[10] H.M. Frost, "'Wolff's Law and bone's structural adaptations to mechanical usage: an overview for clinicians," *The Angle Orthodontist*, vol. 64, no. 3, October, pp. 175-188.

[11] S. Pina, J.M. Oliveira and R.L. Reis, "'Natural-Based Nanocomposites for Bone

Tissue Engineering and Regenerative Medicine: A Review," *Advanced Materials*, vol. 27, no. 7, pp. 1143–1169.

[12] Sigma Aldrich, "'MC3T3-E1 Cell Line from mouse | Sigma-Aldrich,".

[13] Anonymous "'MC3T3-E1 Subclone 4 ATCC ® CRL-2593™ Mus musculus bone/calv,".

[14] COMSOL, "'Acoustic-Structure Interaction,".

[15] Y.1. Sugawara, H. Kamioka, T. Honjo, K. Tezuka and T. Takano-Yamamoto, "'Three-dimensional reconstruction of chick calvarial osteocytes and their cell processes using confocal microscopy." *Bone*, vol. 36, no. 5, May, pp. 877-83.

[16] Sugawara, Ando, Kamioka, Ishihara, Murshid, Hashimoto, Kataoka, Tsujioka, Kajiya, Yamashiro and Takano-Yamamoto, "'The alteration of a mechanical property of bone cells during the process of changing from osteoblasts to osteocytes," *Bone*, vol. 43, no. 1, pp. 19-24.